# NON-LINEAR VARIABILITY IN GEOPHYSICS

## Scaling and Fractals

edited by

D. SCHERTZER AND S. LOVEJOY

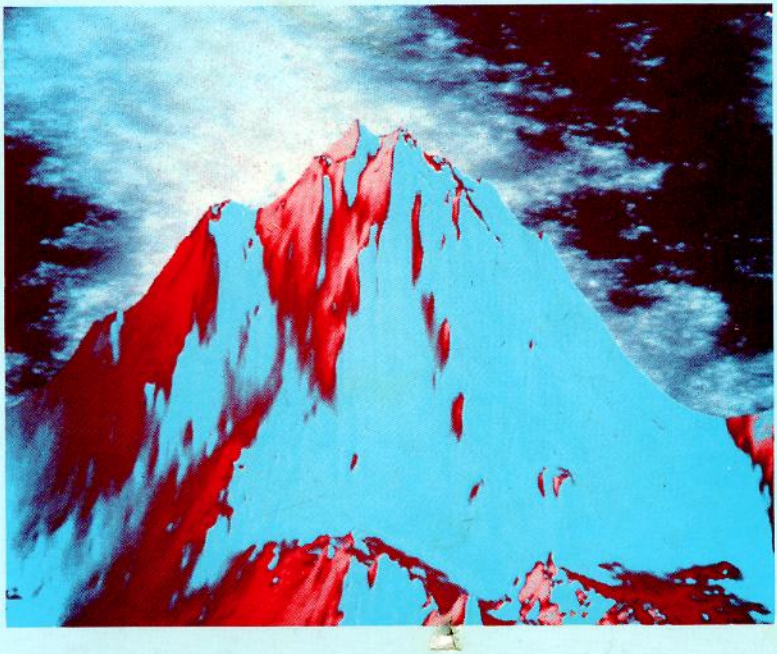

# CONTINUOUS MULTIPLICATIVE CASCADE MODELS OF RAIN AND CLOUDS

J. Wilson, D. Schertzer*, S. Lovejoy
Physics Department,
McGill University,
3600 University st., Montréal, Québec
Canada, H3A 2T8,

ABSTRACT. Early scaling stochastic models of cloud and rain fields were designed to respect an unrealistically simple scale invariant symmetry called "simple scaling" or "scaling of the increments", involving a single fractal dimension. These monofractal processes were produced by summing a large number of random structures: pulses and/or wave packets (depending on whether the model was based in real or Fourier space) and in spite of this extreme simplification yielded simulations of cloud fields with some realistic features including texture, clustering, bands and intermittency. The linear (additive) nature of these processes is however intrinsically related to the fact that they have a single fractal dimension and is in sharp contrast with the non-linear nature of the true dynamical processes and with the observed multiple fractal dimensions of the fields. From this perspective, even the relatively simplified case of stochastic modeling of passive clouds - i.e. passively advected by a turbulent velocity field - is already beyond the scope of linear stochastic approaches, because of the statistical implications of the highly non-linear distortion of the concentration field by the turbulent velocity field. Focusing on this problem, we show how to build up models corresponding to coupled cascade processes, non linearly conserving the fluxes of energy and concentration variance. These cascades, have generally been based on a series of highly artificial discrete steps, are here taken to their continuous limit. Continuous cascades are not only far more realistic than their discrete counterparts, they also admit universality classes characterized by 2 parameter generators. This means that a simple (dynamical) generator describes the entire multifractal spectrum rather than an infinite number of (geometric) dimension parameters. We also show how to numerically simulate such processes with both Gaussian and Lévy generators as well as how to perform rescaling iteration on the results which is scale invariant "zooming" procedure.

## 1. INTRODUCTION

In recent years, many efforts have been made to tackle the problem of extreme variability and intermittency in turbulent atmospheric fields. Interest in this problem comes from both geophysical observations and from the emerging dynamical understanding of the importance of chaotic behaviour. From the empirical point of view, our knowledge of the relationship between the various fields obtained from different remotely sensed or in-situ measurements is somewhat limited as shown for instance, by the problem of infering rain or cloud liquid water fields from radar reflectivities or satellite radiances (e.g. radar calibration by rain gauge networks, the "albedo-paradox", etc.; see various papers in this volume). Even the relationship between similar sets of data spatially averaged at different resolutions, is not at all trivial, especially since the different fields are generally non-linearly related.

From the dynamical point of view, the understanding of the ("meso-scale") inner limit in numerical weather prediction (NWP) models is often the aspect of the extreme variability that is most seriously considered. However, understanding the resolution dependence of atmospheric fields is important well beyond the problem of NWP modelling. Even if we had complete information about the $10^{27}$ - odd

*EERM/CRMD, Météorologie Nationale, 2 Av. Rapp, Paris 75007, France



*D. Schertzer and S. Lovejoy (eds.), Non-Linear Variability in Geophysics*, 185–207.

velocity, pressure and other meteorological elements that are required to specify the state of the atmosphere down to the dissipation scale (which is roughly one millimeter), we would still not know what to do with it, i.e. we would still not have "understood" the weather, nor be in a position to meaningfully describe the atmosphere - we would still require appropriate macroscopic (statistical) concepts. Even within the context of the existing relatively limited number of degrees of freedom in NWP models (typically, about $10^6$) sophisticated initialization procedures are required, which smooth out (if not literally truncate), small scale atmospheric structures. In actual fact the physically relevant number of degrees of freedom is much smaller since most of the dynamics occur in small fraction of the total available space i.e. the processes occuring in only a small number of grid points will be decisive for the evolution of the system. This suggest that NPW models would have much to gain by being able to "zoom" into active regions (this idea is already somewhat exploited in "nested" models in which high resolution regional models are placed inside larger global models). The systematic rescaling procedure we study here provides the proper theoretical framework for these problems and suggests possible operational procedures in the near future.

Furthermore, NWP-modelers use ad hoc pseudo-viscosities to dissipate energy at the inner scale to avoid a constant accumulation of energy (and hence "explosion"). These models can therefore not deal directly with processes in which energy is transfered from smaller physical scales up to grid scales. A related problem is that of sensitive dependence on initial conditions which is a general feature of atmospheric models, and presumably also of the atmosphere. Because of these (and other) limits to the deterministic dynamical approach it is of interest to study other types of models which are primarily aimed at producing realizations with realistic statistical properties. These models are phenomenological in the sense that while they may respect many of the symmetries (conservation laws) of the deterministic dynamical equations, but they are not (yet!) linked to them in a more fundamental way. They have an important role to play in better understanding the statistical properties of the deterministic equations, and perhaps by forming the starting point for a new dynamical-stochastic approach to the problem (e.g. "flux dynamics" in Schertzer and Lovejoy (this volume)).

We start from the idea that atmospheric fields featuring strong variability over wide ranges in scale should not be artificially split apart into large and small scales. We seek rather to study their overall statistical nature over a wide range of scales in relation with their dynamics. For the moment, one has to use all available means, including the investigation of their dimensions, symmetry properties, and topology, their mathematical nature (the singular limit of their support differentiability) their statistical properties (multiple scaling exponents, extreme variability, stationarity) and their general links to the atmosphere dynamics.

The most promising stochastic models are those physically based on the cascade phenomenology of the atmosphere and its governing equations. This makes possible the development of stationary processes applicable to fields conserving their flux densities. In the present paper we limit ourselves to continuous multiplicative cascade models, applied to passively advected clouds. This velocity field is related to the energy field obtained by a scale invariant multiplicative cascade, which is the continuous generalization of the now familiar discrete cascade models[1] (see e.g. Lavallée et al., this volume). Before giving the details of the construction steps, we will investigate the physics of passive scalar fields. Finally, we give the details of the numerical implementation of the latter process.

## 2. PHYSICAL BASIS OF MULTIFRACTAL PASSIVE SCALAR CLOUD SIMULATIONS

We consider the simplest type of clouds which result from the passive advection of water concentration ($\rho$) by a velocity field ($\underline{v}$):

$$\frac{\partial \underline{v}}{\partial t} + (1\text{-}P(\nabla))\, \underline{v}\cdot\nabla\, \underline{v} = f + \nu\nabla^2\, \underline{v} \qquad (2.1)$$

$$\frac{\partial \rho}{\partial t} + \underline{v}\cdot\nabla\, \rho = f' + \kappa\nabla^2\rho$$

[1] It is worth noting that although Mandelbrot (1972) apparently used Fourier series in certain numerical simulations of cascades, he did not investigate the continuous limit (Fourier transforms). Since the universal properties of multiplicative cascades appear only in this limit, this explains his recent (Mandelbrot, 1989) strong statement that there are no universal dimension functions (or, equivalently, generators) for such cascades.

Where[1] $P(\nabla) = \nabla^{-2}\nabla_i\nabla_j$. First we note that the nonlinear terms $((1-P(\nabla))\ \underline{v}\cdot\nabla\ \underline{v}\ ,\ \underline{v}\cdot\nabla\ \rho)$ of both the incompressible Navier-Stokes equations and the equation of (passive) advection dynamically conserve the fluxes of energy and scalar variance (having densities $\varepsilon$ and $\chi$ respectively). This conservation is simply expressed in terms of the fluxes of energy and scalar variance:

$$\varepsilon = -\,\partial\langle v^2\rangle/\partial t = \text{constant}$$
$$\chi = -\,\partial\langle \rho^2\rangle/\partial t = \text{constant} \qquad (2.2)$$

Furthermore, in Fourier space the non-linear terms are heavily weighted to interactions involving neighboring wavenumbers- thus the energy flux is mainly transfered from one scale to a neighboring scale, hence the Richardson- Kolmogorov idea of energy cascading from large to small scales. From here, various phenomenological arguments (which boil down to dimensional analysis) leads to the well-known Kolmogorov scaling (power law) spectra. These all rely on the invariance of the equations under the dilation transformation $\underline{x}\to\underline{x}/\lambda$, $\underline{v}\to\underline{v}/\lambda^H$ and $\rho\to\rho/\lambda^{H'}$ (here and below, the prime refers to the passive scalar cascade). This scaling leads to the following relations for the "fluctuations" at scale $l$ of the fields $\underline{v}$ and $\rho$ (these fluctuations can be characterized for example by the standard deviations of the differences, or increments in v and $\rho$ at points separated by distance $l$) denoted $\Delta v(l)$ and $\Delta\rho(l)$. Furthermore, dimensional analysis applied to $\chi$ and $\varepsilon$ implies H=H'=1/3, or:

$$\Delta v(l) \approx \varepsilon^{1/3}\, l^{1/3}$$
$$\Delta\rho(l) \approx \varphi^{1/3}\, l^{1/3} \qquad (2.3)$$

This invariance leads to power law spectra $E_v(k) \sim k^{-\beta}$ and $E_\rho(k) \sim k^{-\beta'}$ which are respectively the power spectra for the velocity and passive scalar fields (depending on k, the wave number: $k\approx 2\pi/l$) and $\beta=2H+1$ and $\beta'=2H'+1$ since the power spectrum is the Fourier transform of the autocorrelation function:

$$E_v(k) \approx \varepsilon^{2/3}\, k^{-5/3}$$
$$E_\rho(k) \approx \varphi^{2/3}\, k^{-5/3} \qquad (2.4)$$

where $\varphi = \chi^{3/2}\,\varepsilon^{-1/2}$ is the flux resulting from the nonlinear interactions of the velocity and water. Note that the above are scale invariant since their forms are conserved under the dilation $k\to k\lambda$).

The values H=H'=1/3 and $\beta=\beta'=5/3$ were obtained only because the first (h=1) moment of the flux is conserved. So, the question arises as to what should be the scaling exponents for the orders $h\neq 1$. And as far as scale invariance of equations 2.1 is concerned, a different value is possible for every (integer or non integer order) moment hence the terminology of "multiple scaling". This can be expressed for local density values of the field, called (which, at homogeneity scale $l$) with the following scaling laws:

$$\langle \varepsilon_l^h \rangle \sim l^{-(h-1)C(h)}$$
$$\langle \chi_l^h \rangle \sim l^{-(h-1)C'(h)} \qquad (2.5)$$

It can be shown that in general the functions C(h)=d-D(h) and C'(h)=d-D'(h) are codimension functions[2], where D(h), D'(h) are the general multifractal dimensions of the various moments of the process. In the simplest case of a process having a unique fractal codimension C(1), all the various moments of the physical quantities have scaling exponents which are linearly related (differing only by the factor (h-1)), and in this restrictive situation all moments scale the same way. Aside from this, when the functions C(h) and

[1]This form of the equations is obtained after the pressure term is eliminated under the assumption of incompressibility.

[2]A co-dimension is the difference between the dimension d of the embedding space and the fractal dimension of the set of interest.

C'(h) are nonlinear in h we obtain a full spectrum of scaling exponents which are all consistent with the scale invariance of the leading dynamical equations. Since higher order moments single out and enhance the more intense regions of the field, multiple scaling simply expresses the fact that the most intense regions of the field will scale differently than the weak regions. So, in the case of multiple scaling (which was first proposed by Kolmogorov (1962) and Obukhov (1962)) who this singular statistical behaviour was later proposed by Parisi and Frisch (1985), analyzed this in term of singularities of various order $\gamma$ in the local energy-flux density field: $\varepsilon_l \geq l^{\gamma}$. These singularities are indeed consistent with the multiple scaling behaviour and they are the expressions of the minimal rate of divergence of $\varepsilon_l$ as $l$ tends to zero, this will be discussed in more details in section 3.2 a spectrum of scaling exponents for the moments implies a hierarchy of singularities.

## 3. CONTINUOUS CASCADE MODELS

### 3.1. General outline

In a series of attempts to take into account the highly variable (intermittent) nature of the $\varepsilon$, $\chi$ fields, a considerable literature on cascade processes has developed. Nearly without exception, the cascades discussed in the literature have been discrete, i.e. eddies divided into integral numbers of sub-eddies, each an integral fraction of size of the parent (see appendix A for an introductory discussion). Discrete cascades are unsatisfactory models of physical phenomena for many reasons, perhaps the most obvious being the multitude of artefacts such as square remnants and ghostly lines due to the explicit splitting by an (integer) factor $\lambda$ of the basic rectangularly shaped eddies.

It is helpful to recall some elements of probability theory. For a random variable g, denote by $\varphi_g(h)$ the "second Laplacian characteristic function of g";

$$\langle e^{hg} \rangle = e^{\varphi_g(h)} \tag{3.1}$$

then, if $g_1, g_2, \ldots g_n$ are independent random variables, then:

$$\varphi_{\sum g_i}(h) = \sum_i^n \varphi_{g_i}(h) \tag{3.2}$$

In particular, consider g to be a sinusoid, wavenumber $\underline{k}$, amplitude $f(\underline{k})u_{\underline{k}}$, phase $\phi_{\underline{k}}$, where u is a Gaussian random variable with $\langle u^2 \rangle = \sigma^2$, $\langle u \rangle = 0$, $\phi_{\underline{k}}$ is a random variable uniform of $[0,2\pi]$. In section 3.5 and in appendix B (see also appendix A of Schertzer and Lovejoy, this volume) we consider the more mathematically involved case where u is an infinite variance Lévy random variable. We obtain:

$$g_{\underline{k}} = e^{i\underline{k}\cdot\underline{x}} f(\underline{k}) u_{\underline{k}} e^{i\phi_{\underline{k}}} \tag{3.3}$$

$$\varphi_{g_{\underline{k}}}(h) = -\frac{\sigma^2}{2} h^2 |f(\underline{k})|^2$$

Using the addition property (eq. 3.2, generalized from sums to integrals), we obtain:

$$\varphi_{\int g_{\underline{k}} d\underline{k}}(h) = -\frac{\sigma^2}{2} h^2 \int |f(\underline{k})|^2 d\underline{k} \tag{3.4}$$

Eq. 3.4 makes it clear why the choice of a Gaussian is judicious - the central limit theorem shows that , under the infinite sum limit above a Gaussian limit will be obtained (as long as the random variables are chosen independently and have a finite variance). In order to model a multiple scaling (multifractal) field, recall that we seek a field $\varepsilon_\lambda$ with resolution (finest scale) $\lambda$, (c.f. eq. 2.5) satisfying:

$$\langle \varepsilon_\lambda^h \rangle = \lambda^{K(h)} \tag{3.5}$$

Rewriting this slightly:

$$\langle e^{h \ln \varepsilon_\lambda} \rangle = e^{K(h) \ln \lambda} \tag{3.6}$$

Where K(h) is the exponent characterizing the scaling of the $h^{th}$ moment. It is therefore obvious that $K(h)\ln\lambda$ is the second Laplacian characteristic function of $\ln\varepsilon_\lambda$. We therefore construct a stochastic model for $\ln\varepsilon_\lambda$ by using eq. 3.4 and adding random sinusoids with wavenumbers between 1 and $\lambda$ with $f(\underline{k})$ chosen so that:

$$\int_1^\lambda |f(\underline{k})|^2 d^d\underline{k} = n_d \int_1^\lambda |f(\underline{k})|^2 |\underline{k}|^{d-1} d|\underline{k}| = \ln\lambda \tag{3.7}$$

Where $n_d$ is a constant depending on the dimension of space that results from the angular integration ($=1, 2\pi, 4\pi$ in d=1,2,3 respectively). Since $n_d |f(\underline{k})|^2 |\underline{k}|^{d-1}$ is simply the spectral energy E(k), the above is equivalent to stating that the energy spectrum of the logarithm of a multifractal field must be a "1/f noise" (i.e. have a wavenumber spectrum $E(k) \propto |\underline{k}|^{-1}$). The final ingredient in a continuous multifractal cascade is the determination of the proportionality constant in eq. (3.7) by imposing the conservation condition $\langle \varepsilon_\lambda \rangle = 1$. Using eq. (3.5) this implies K(1)=0, which can be achieved by dividing an unnormalized $\varepsilon_\lambda$ by $\langle \varepsilon_\lambda \rangle$. If $K_u(h)$ is unnormalized, then the corresponding normalized second characteristic function is $K(h)\ln\lambda$ with $K(h)=K_u(h)-hK_u(1)$.

Putting together all the above elements using the normalization as indicated, we can now give the following method for modelling a continuous cascade in d dimensional space. We choose:

$$f(\underline{k}) = |\underline{k}|^{-d/2} n_d^{-1/2} \tag{3.8}$$

with u, Gaussian: $\langle u^2 \rangle = 2C_1$ (i.e. $C_1 = \sigma^2/2$) and $\langle u \rangle = 0$.

These choices, followed by Fourier transformation, and exponentiation will lead to a field that requires division by the normalization factor $\lambda^{\sigma^2/2}$. The resulting normalized field will have $K(h)=C_1(h^2-h)$. The codimension function corresponding to $h^{th}$ order moments is $C(h)=K(h)/(h-1)= C_1 h$, hence the value $C_1$ is the codimension of the mean field (i.e. for h=1).

It should be noted at this point that the requirement that the Laplacian characteristic function (eq. 3.6) must converge restricts the possible probability distributions of the random variables. This is not surprising since if the random variable $\ln\varepsilon_\lambda$ has sufficiently frequent large positive values, the left hand side of eq. 3.6 may not converge for any $h \geq 0$. In the Gaussian case discussed here, the extreme values are very rare and there is no difficulty, however, in infinite variance Lévy cases, the extreme tails of the probability distributions are generally algebraic (exponent $-\alpha$) and eq. 3.6 will diverge. The only exceptions are the "extremal" (maximally asymmetric) Lévy distributions which can be chosen so that their positive values have weak (exponentially decaying) fluctuations with only their negative values being algebraic. These are the only Lévy distributions with $\alpha<2$ that yield convergence and are discussed in more detail in appendix B.

### 3.2. Numerical simulation of two dimensional $\varepsilon_\lambda$ fields with Gaussian generator ($\alpha=2$)

One-dimensional simulations are sufficient for the study of many of the statistical properties of the cascade. However, if we are interested in the ("coherent") structures of the multifractal field, it is clearly more interesting to produce simulations in two or more dimensions. Ultimately, four dimensional (space-time) simulations would provide information on temporal evolution and hence on the predictability of the fields.

In the Gaussian case, the implementation is straightforward. We use Gaussian white noise (mean zero, variance given below) distributed over a rectangular grid in 2D Fourier space up to the maximum excited wave number $2\pi\lambda/l_0$ which corresponds to the largest scale of homogeneity (=smallest scale of variability) $l_0/\lambda$. The variance $\langle u^2 \rangle = 2C_1$ is chosen so that the codimension function is:

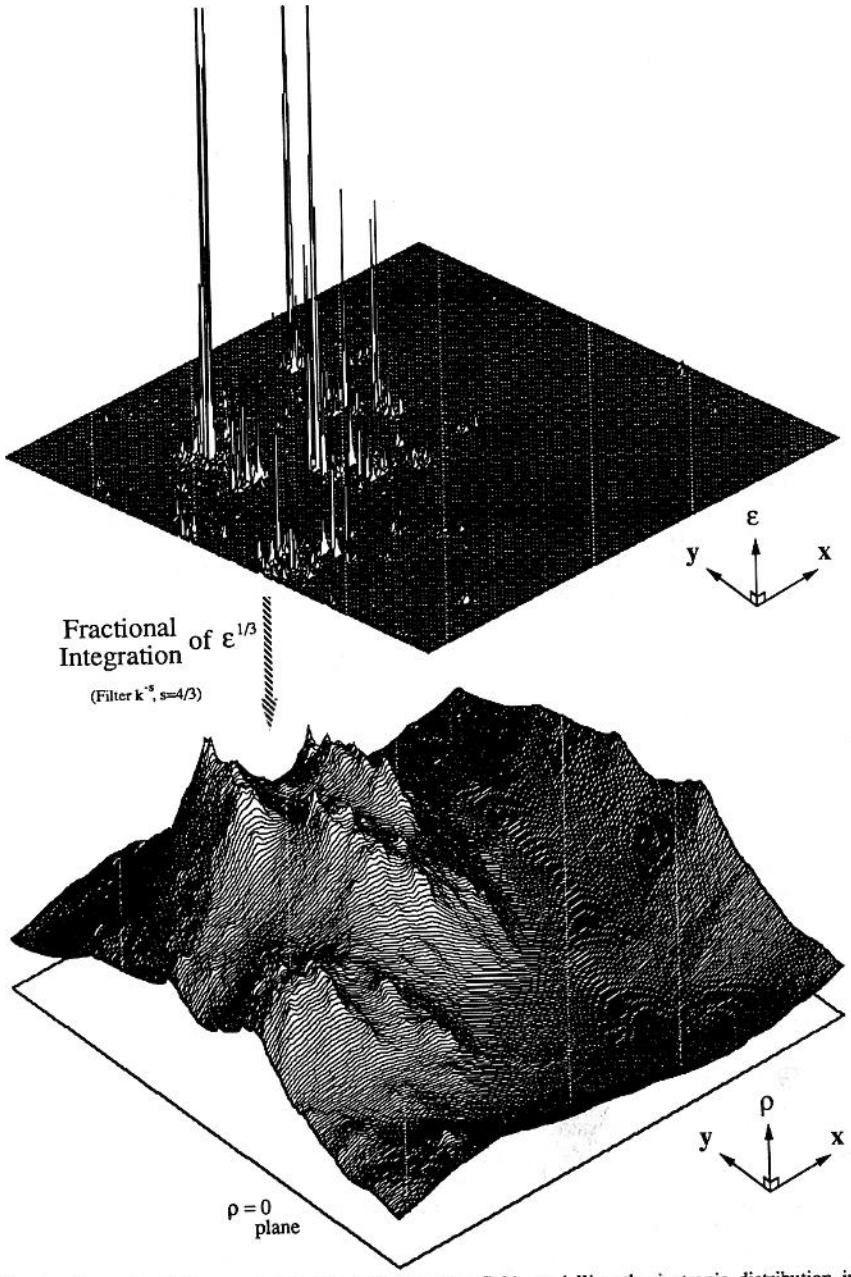


Fig. 1: Example of the generation of a passive scalar field, modelling the isotropic distribution in two dimensions (i.e. cut in the horizontal plane) of the concentration of cloud water content (at the bottom), from the corresponding energy flux density field (upper field). In this perspective plot, done on a $2^8 x 2^8$ pixel grid, the height (in the vertical) of the structures represents respectively the values of energy $\varepsilon$ and concentration $\rho$. The transformation from the former to the latter field is insured by a scale invariant smoothing operation called the fractional integration applied to the one third power of the energy field. The energy flux density field is obtained by a continuous multiplicative cascade using a Gaussian generator ($\alpha$=2) and has a fractal dimension of $D_1$=1.2 associated with the first order moment ($C_1$=2-D[h=1]=0.8).

$$C(h) = C_1 h \tag{3.13}$$

Finally, we exponentiate the Fourier transform (FFT) of the field. The normalization of the resulting $\varepsilon_\lambda$ field must take into account the fact that the continuous integral is replaced by a discrete sum, and this implies a correction in the form of the Euler constant $\gamma_e$=0.57..., since

$$\left( -\int_1^n \frac{dx}{x} + \sum_{i=1}^{n} \frac{1}{i} \right) \xrightarrow[n\to\infty]{} \gamma_e \tag{3.14}$$

The upper part of figure 1 shows a two dimensional energy field simulation having a (1/f) Gaussian generator ($\alpha$=2) and resulting from a continuous multiplicative cascade done over a $2^8$x$2^8$ pixel grid. As an illustration, an example of the needed Gaussian subgenerator field is provided at the top of figure 8 (which is simply a symmetric unitary Gaussian white noise). So, we have chosen in the simulation $C_1$ = 0.4, such that fractal dimension associated with the mean of the field is d-$C_1$ = D(h=1) = 1.6.

3.3. Simulation of two dimensional cuts passive scalar clouds- fractional integration

To model passive scalar density field $\rho$, we require both $\varepsilon$, $\chi$.which will generally be coupled (dependent) cascade quantities. $\rho$ is then determined from $\Delta\rho \approx \varphi^{1/3} l^{1/3}$ where $\varphi = \chi^{3/2}\varepsilon^{-1/2}$ (see section 2).

The simplest (albeit extreme) procedure for obtaining a $\varphi$ field is to assume that the energy and passive scalar variance fluxes are completely correlated, ($\varepsilon \propto \chi$) hence $\Delta\rho \approx \chi^{1/3} l^{1/3}$ or alternatively, $\Delta\rho^3 \approx \chi l$. The factor $l$ represents an integration of order one which can easily be accomplished in Fourier space by dividing by $|\underline{k}|$. Hence, in order to produce a field with the correct scaling properties, we Fourier transform $\chi$, divide by $|\underline{k}|$, transform back into real space, and then take the cube root. These operations act only on the amplitudes of the field, leaving the phases entirely unchanged, and has the main mathematical effect of a scale invariant smoothing operation which establishes the required spectrum for the field of concentration $\rho$.

The only numerically delicate part of this scheme is the need for some care in the memory management. Since the procedure uses purely real physical fields, one should take advantage of this when performing the fast Fourier transform (FFT) which is the time limiting step in the simulation. Large scale simulations are easily performed. The example given in figure 1 shows the resulting concentration field over a $2^8$x$2^8$ pixel grid simulated on a personal computer. The generation of a passive scalar field proceeds in the same way for any other value of $\alpha$ ($\alpha$<2) once the energy field is provided (see below).

Numerical implementation of the process is straightforward without any special difficulty except for the use of discrete fast Fourier transforms which have their own limitations. Possible alternative methods might involve use of "wavelet" transforms, together with windowing techniques. Even without zooms (see below) very large simulations are possible (perhaps up to $512^3$ on Cray 2 supercomputers). If we assume that the homogeneity scale of the process corresponds to the viscous scale =1 pixel, then $Re_1$ = 1 and using $Re_l = v\, l/\nu \approx \varepsilon^{1/3} l^{1/3}/\nu$ where $\nu$ is the viscosity. Hence:

$$Re_l \approx \left(\frac{\varepsilon^{1/3} l^{4/3}}{\nu}\right) \left(\frac{\varepsilon^{1/3}}{\nu}\right)^{-1} Re_1 \approx l^{4/3} \tag{3.15}$$

Hence, using $l$ =512, we have $Re_l \approx 4000$ which compares very favorably, with the largest direct numerical simulation of Navier-Stokes, for which $Re_l \approx 100$ (on a 128X128X512 grid). However the real advantage of these models is the possibility of zooming outlined below which allows us to simulate over effectively unlimited range scale.

Examining figure 1, one notices the periodic character due to the Fourier treatment. The latter is more evident in the case of the concentration field rather than for the energy field since the smoothing by fractional integration forces the spectral amplitude of a given structure of the energy field to slowly extend its influence over the neighboring points of the grid. If the structure is near the border the corresponding effect appears on the other side. To avoid this artifact, one may choose to eliminate a small strip near each border or use one of the numerous window filtering techniques with a view to minimizing the effect on the spectrum (which is biased anyway at high wave numbers due to both aliasing and the periodicity of the Fourier transform).

### 3.4. Normalized zoom sequences

Although unrealistic, discrete cascades have the interesting property that by a simple iteration process we multiplicatively insert more and more small scale detail: we "zoom" into smaller and smaller regions. In this sub-section we show how to perform such zooms on continuous cascades (see Wilson et al. (1986) for more discussion on zooming).

The main principle in the actual implementation of zooming is first, to retain a small square window from the original two-dimensional energy field, and second, to map this new field on the original grid by enlarging by a factor $\lambda_z$, the values retained being repeated the appropriate number of times on the neighboring pixels. For the sake of simplicity we will use in the following a zoom factor $\lambda_z=2$, so that when we double, each pixel becomes a 2x2 field element. The last step is simply the multiplicative modulation of smaller structures to refine the details of the field by "reactivating" all the newly available degrees of freedom at the new resolution. For simulations done on a $\lambda x\lambda$ pixel grid, since we retain $1/\lambda_z$ of the former field, this additional information represents then $\lambda x\lambda(1-1/\lambda_z)$ degrees of freedom, or, for $\lambda_z=2$, exact one half.

The insertion of the high wavenumber (small scale) details is performed in a multiplicative way with the appropriate normalization. To do this, a new field is created in the same way as previously except that the range in scales is the exact complement of that of the doubled field. In Fourier space a cascade is performed in a spectral band spanning $2\pi\lambda_z/l_0 \leq |\underline{k}| \leq 2\pi/l_0$. This partial field is then transformed back to physical space and exponentiated with a normalization corrected this time by the zoom factor in such a way that all points of this new field act as independent multiplicative increments. Since both fields have the same spatial extent (the same number of degrees of freedom), the final modulation is performed by direct point by point multiplication. Thus, the zooming technique applied here, applied multiplicatively in discrete steps yields the same continuous cascade as before, except that we now we have separately modeled the two contiguous ranges of scale related by the zoom factor. A concentration field can be obtained from each of the newly zoomed $\chi$ fields by taking integration of order one as before and then the cube root.

Figures 2 and 3 illustrate three successive zooms with $\lambda_z=2$ on a 256x256 pixel concentration field with a Gaussian generator. The first figure shows the technique applied to the center 128x128 window whose corresponding $\chi$ field is singled out, doubled and then modulated with finer scale structures before being reconverted to a zoomed concentration field. Repeating the process two more times in figure 3, we obtain an enlarged 256x256 view of the former 32x32 centered pixels of the first field, or equivalently after a global factor 8 zoom (each step of process being repeated recursively) the center window looks as if it were taken from a 2048x2048 primitive field. One can see the signature of the Fourier transforms by the periodicities introduced in the transformation relating $\chi$ to $\rho$ which is an artifact of the finite Fourier transforms.

This can also be seen with more details in bigger "zooming" simulations (done over a 512x512 grid scale): as in the case of figures 4 and 5 featuring a topographical representation of passive scalar fields with a one iteration zoom; and also: in the case of figures 6 and 7 where we simulate cloud like representations with a three iterations zoom based on a different realization of a normalized Gaussian generator (see legends for details). The imaging procedures used here (ray tracing or logarithmic grey scale) are standard ones applied on multiplicative cascade fields.

The scale invariant zooming technique can be used as a diagnostic tool to check our premises about the correct normalizations involved in all parts of the process both theoretically and numerically. As mentioned earlier, since we are dealing with highly intermittent fields which are multiplicating one each other, any small numerical or other errors lead quickly to numeric overflows.

### 3.5. Simulation of $\varepsilon_\lambda$ fields and passive scalar clouds with Lévy-stable generator ($\alpha<2$)

In this subsection, we describe the modelling of the (non-Gaussian) universality classes involving Lévy distributions with $\alpha<2$. Recall that Lévy distributions are the only limiting distributions for sums of independent, identically distributed (i.i.d.) random variables, and hence are the generalizations of the Gaussian (which corresponds to $\alpha=2$). They are the limit of (appropriately normalized) sums of i.i.d. random variables whose variances are infinite. It is due to this "attractive" property that they form the basis of the universality classes for multiplicative processes (see Schertzer and Lovejoy (this volume) for

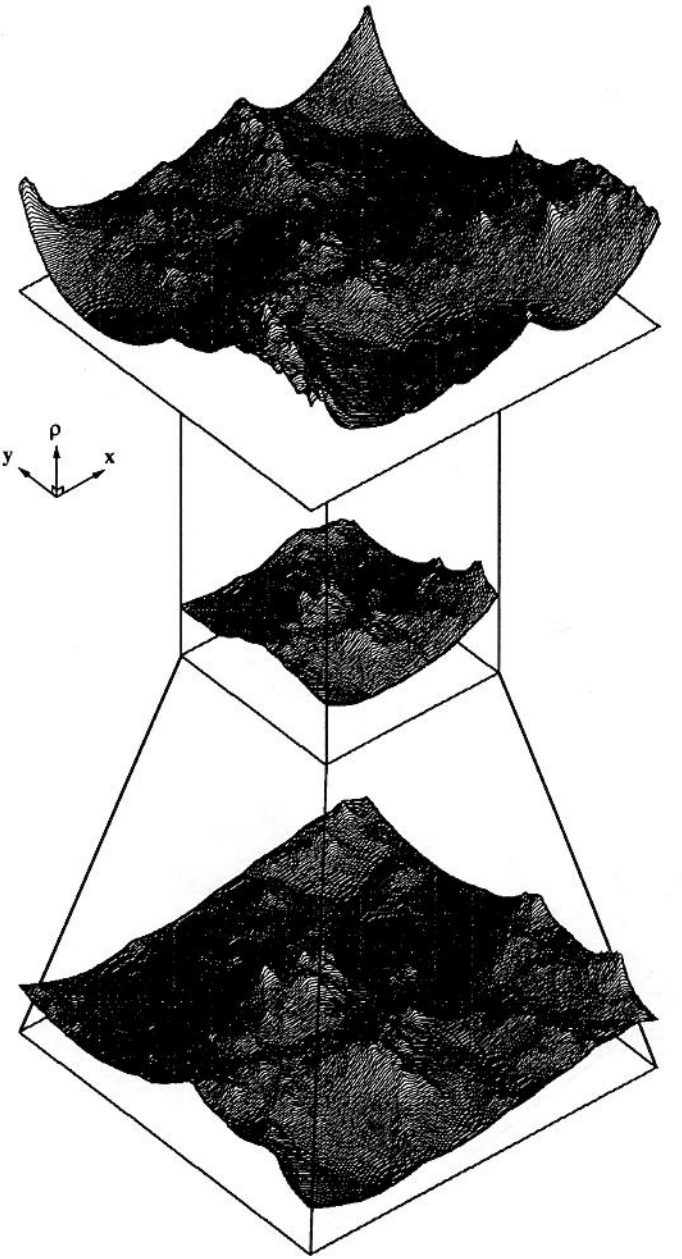


Fig. 2: Illustration of the "zooming" technique applied specifically in the case of the continuous generalization of multiplicative cascades. Here we are zooming by a factor 2 on a 256x256 concentration field issued from a Gaussian generated energy field. The 128x128 window chosen exactly in the center is mapped onto the former resolution where all the newly available degrees of freedom are reactivated. The adjunction of small scale details is done in a multiplicative way which is perfectly coherent with the cascade principles (see text). This illustrates the equivalent discrete step of the former discrete cascades.

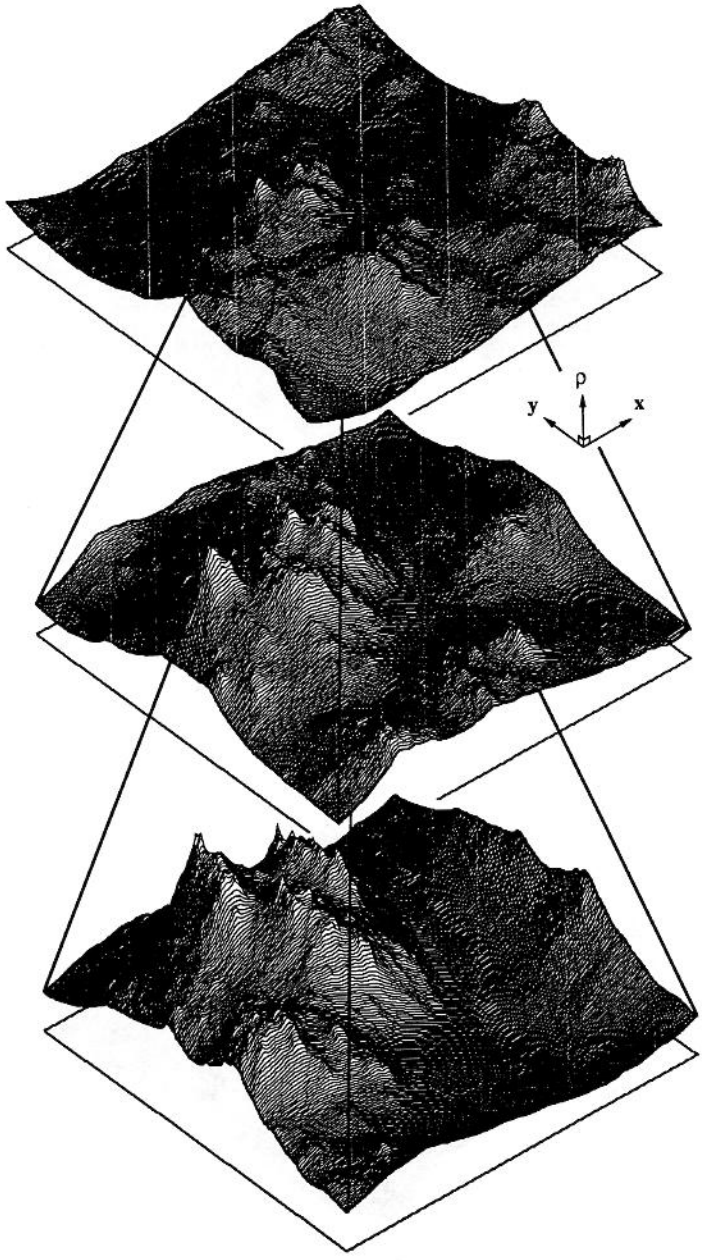


Fig. 3: Examples of generation of two other daughters concentration fields as in figure 2. Repeating here the process of "zooming" in the cascade, by pushing down the inner scale limit two more times with factor 2 zooms, we obtain then a widened 256x256 view of the former 32x32 centered pixels of the first concentration field of figure 2. Equivalently after a global factor 8 zoom (each step of process being repeated recursively) the center window looks like if it were taken from a 2048x2048 primitive field.

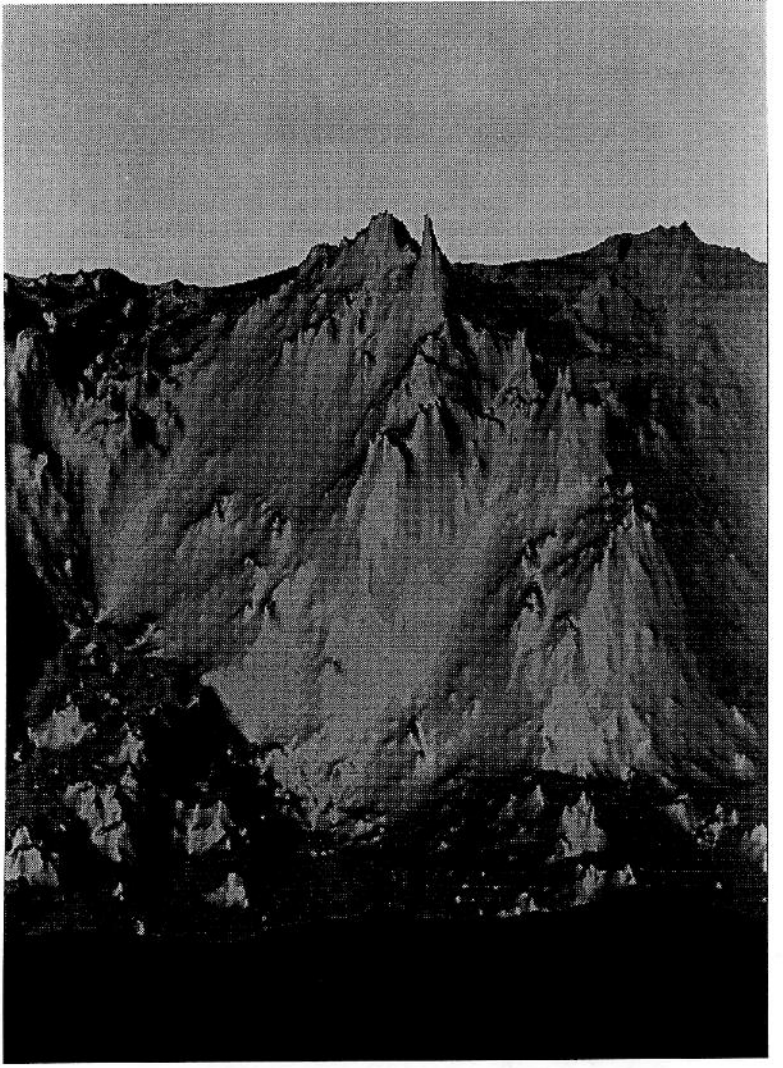

Fig. 4: This figure and the next one illustrate the "zooming" technique applied specifically in the case of the continuous generalization of multiplicative cascades. From this figure to the next one we are zooming by a factor 2 on a 512x512 concentration field issued from a gaussian generated energy field. The 256x256 window chosen exactly in the center is mapped onto the former resolution where all the newly available degrees of freedom are reactivated. The adjunction of small scale details is done in a multiplicative way which is perfectly coherent with the cascade principles. The topographic imaging is done by the application of a ray tracing technique directly to the passive scalar field.

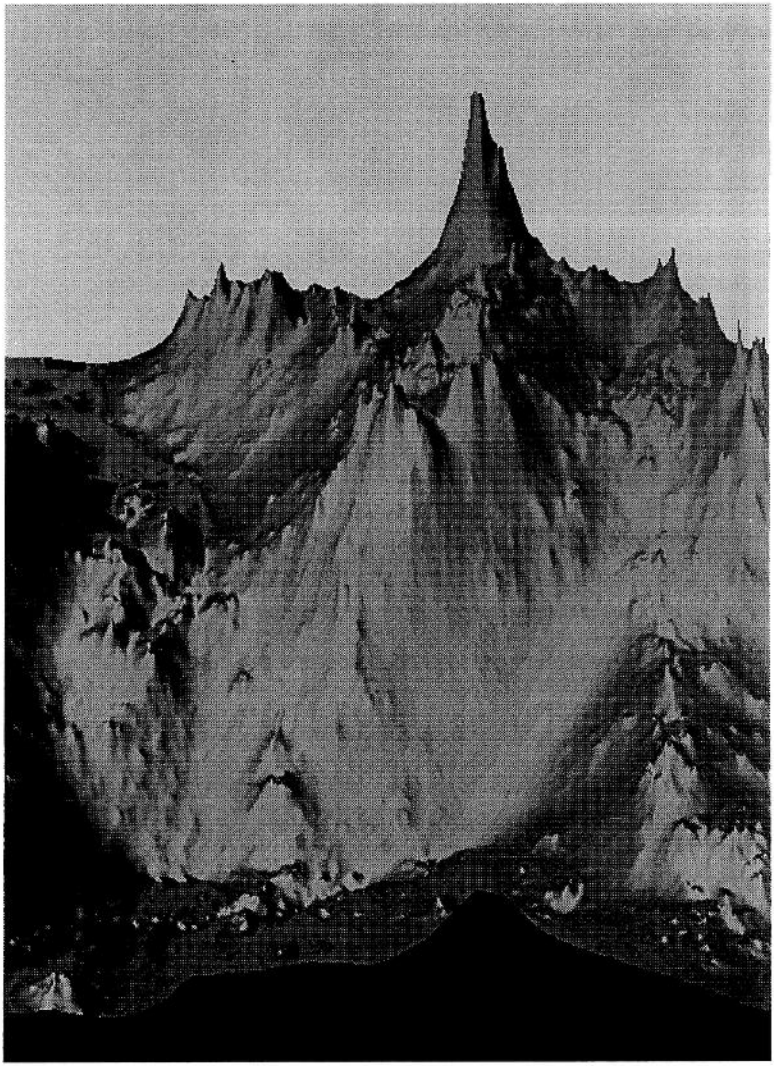

Fig. 5: In this figure we apply the "zooming" procedure to figure 4. The topographic imaging is done again by the application of a ray tracing technique directly to the passive scalar daughter field. Both fields are obtained from a gaussian generator and do feature a fractal dimension of $D_1$=1.2 associated with the first order moment (C[h=1]=2-$D_1$=0.8) .The synthetic topographical field, shown here, is the daughter of the previous one since only small scale details where added in a multiplicative way. Such scale invariant zooms can be iterate easily downward to smaller scales.

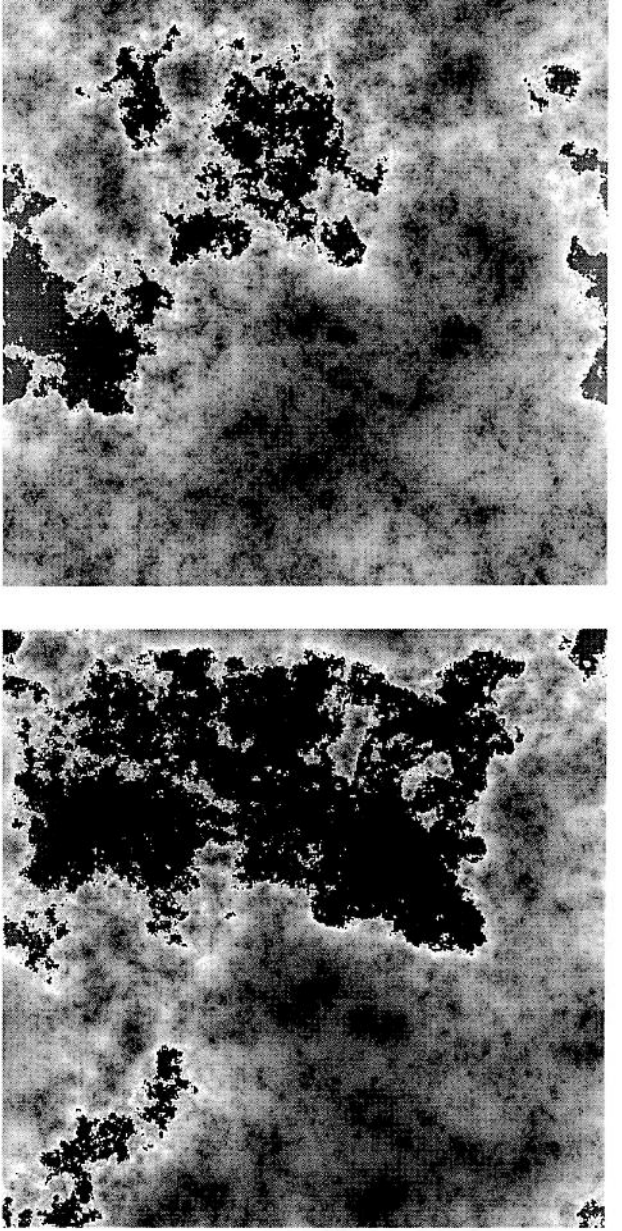

Fig. 6: From top (level 0) to bottom (level 1) we illustrate the "zooming" technique on synthetic cloud fields We are zooming by a factor 2 on a 512x512 concentration field issued from a Gaussian generated energy field which has a fractal dimension of $D_1$=1.2 associated with the first order moment (C[h=1]=2-$D_1$=0.8). The 256x256 window chosen exactly in the center is mapped onto the former resolution where all the newly available degrees of freedom are reactivated. The adjunction of small scale details is done in a multiplicative way which is perfectly coherent with the cascade principles (see text). The cloud imaging effect is obtained by applying a linear grey scale to the logarithm of the field intensities to simulate the action of optical thickness in the cloud field.

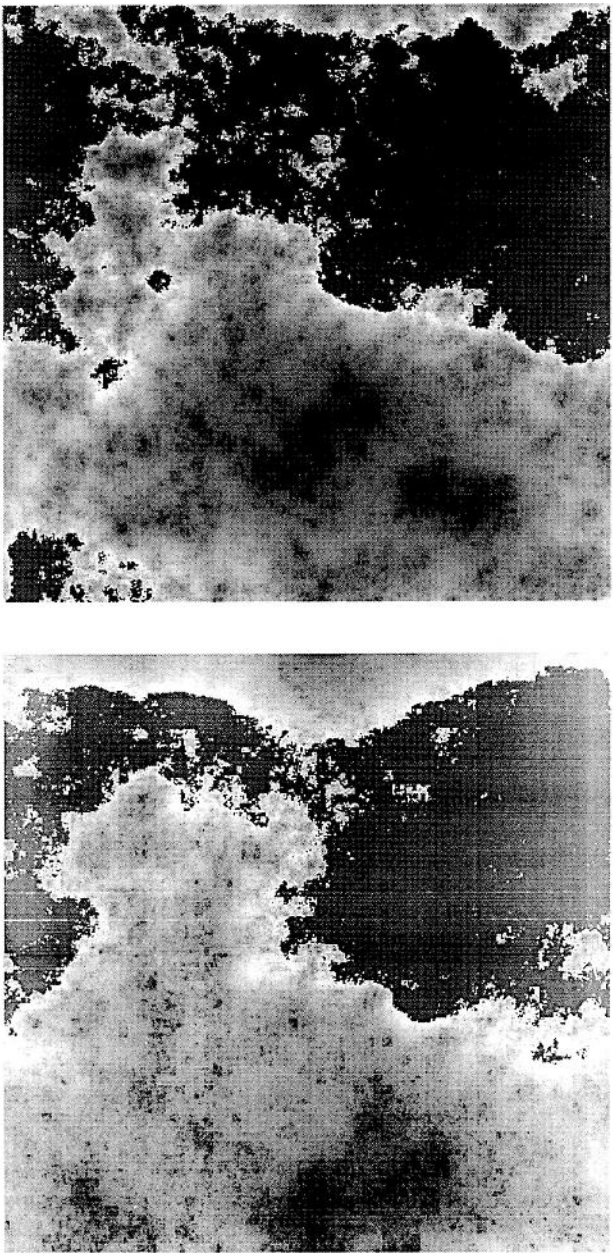

Fig. 7: From top (level 2) to bottom (level 3) we continue the "zooming" procedure of figure.6 The synthetic cloud fields obtained are daughters of the previous ones. The "cloud imaging" is again obtained by applying a linear grey scale to the logarithm of the field intensities to add and simulate the effect of optical thickness to the cloud fields. At each iteration of the "zooming", a threshold under which the sky appears, is determined according to a given level of singularities $\gamma = -.44$ which is chosen to be the same for all fields (level 0 to 3). Such scale invariant zooms can be iterate easily downward to smaller scales.

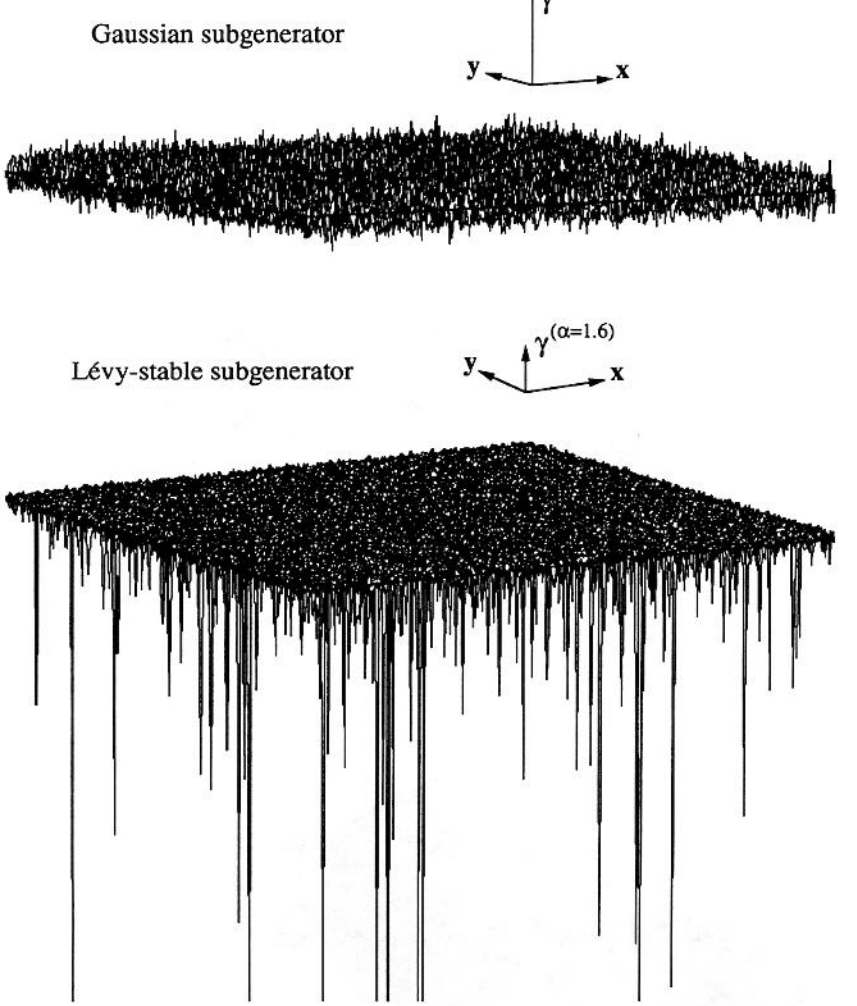


Fig. 8: Two dimensional illustration of two examples of subgenerator field used in continuous multiplicative cascades. The field at the top (a) is made of unitary (mean=0, variance=1) symmetric gaussian ($\alpha$=2) white noises. And, at the bottom (b) the field is obtained by independent sums of 50 centered asymptotically hyperbolic variables (mean=0, $\alpha_h$=1.6) converging towards asymmetrically negative Lévy-stable white noises ($\alpha$=1.6). The perspective plots of the field are depicted on the same physical space, using a $2^8 x 2^8$ pixel grid. The height (in the vertical) of the structures represents respectively the values of the associated random variables, here uniformly independently distributed (the lengths of the appearing vertical axes provide a reference unit). The transformation from this subgenerator to the appropriate 1/f generator field of the cascade requires a fractional integration insured by a $k^{-d/\alpha'}$ (d=2, $1/\alpha'=1-1/\alpha$) filter in fourier space.

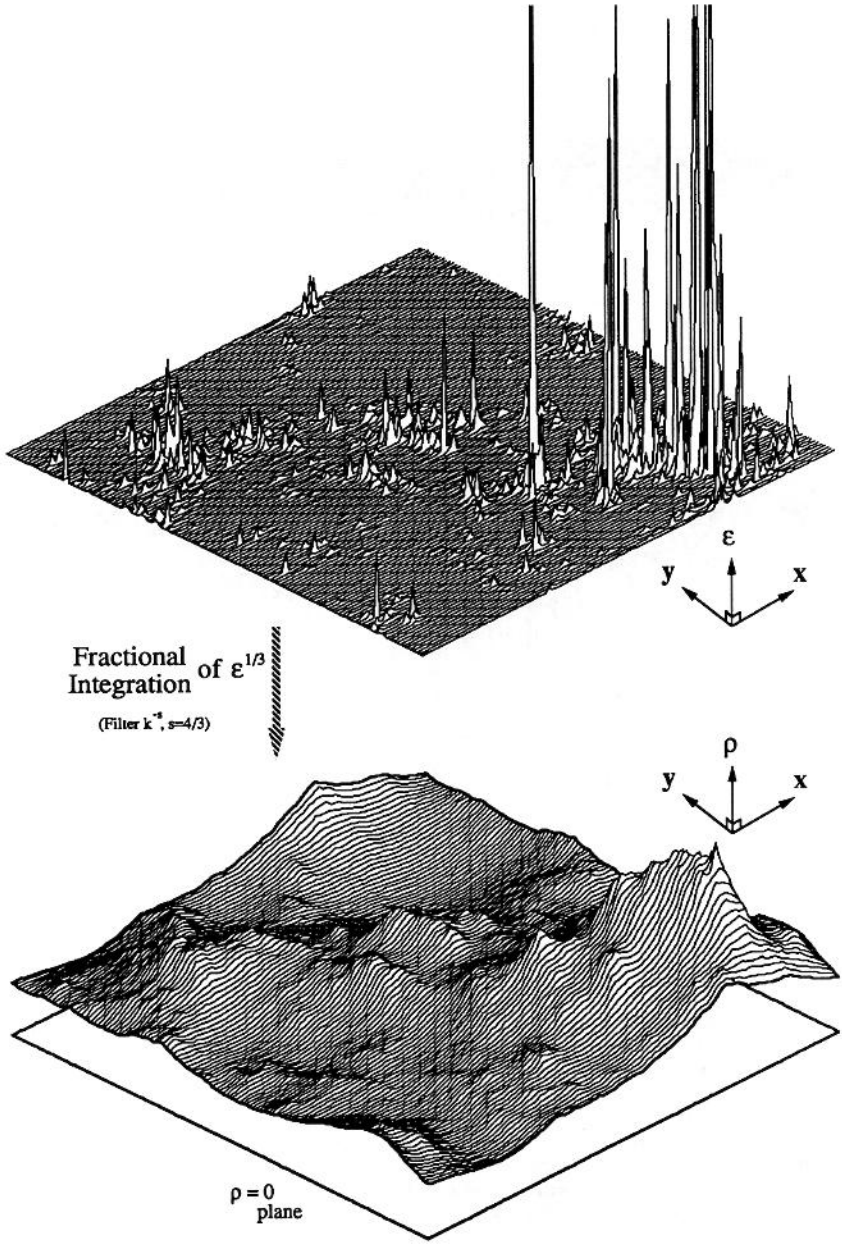


Fig. 9a: Example of the generation of a passive scalar field, modelling the isotropic distribution in two dimensions (i.e. cut in the horizontal plane) of the concentration of cloud water content (at the bottom), from the corresponding energy flux density field (upper field). Here the energy flux density field is obtained by a continuous multiplicative cascade using a 1/f Lévy-stable generator ($\alpha$=1.6) and has a fractal dimension of $D_1$=1.2 associated with the first order moment (C[h=1]=2-$D_1$=0.8). In this perspective plot, done on a $2^7$x$2^7$ pixel grid, the height (in the vertical) of the structures represents respectively the values of energy $\varepsilon$ and concentration $\rho$. The transformation from the former to the latter field requires to do a fractional integration on $\varepsilon^{1/3}$.

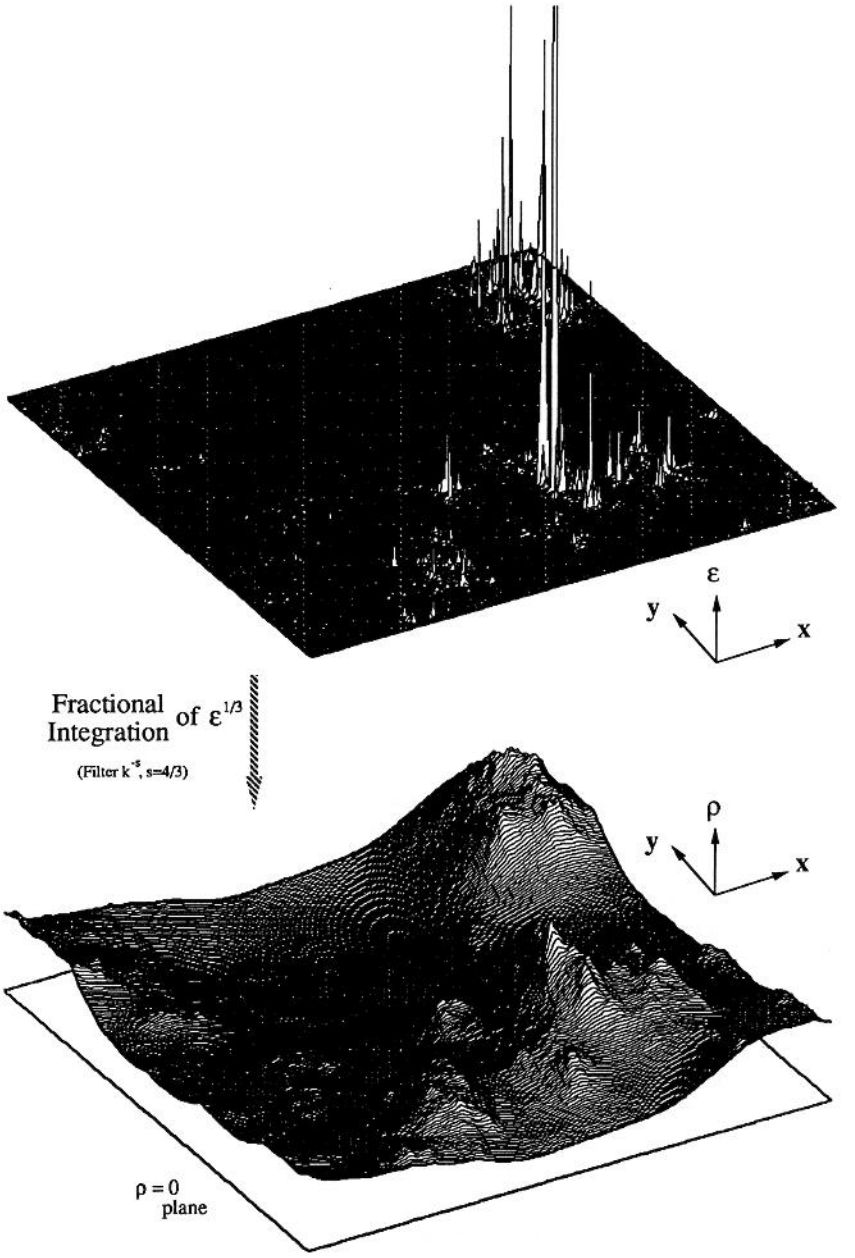


Fig. 9b: Another example of the generation of a passive scalar field, representing also the concentration of cloud water content (at the bottom), from the corresponding energy flux density field (upper field). This latter field, having a codimension associated with the first order moment $C[h=1]=2-D_1=0.8$, comes from the exponentiation of a 1/f generator which is obtained by effecting a fractional integration (filter $k^{-0.75}$) of the Lévy-stable ($\alpha=1.6$) subgenerator field depicted at the bottom of fig.8. In this perspective plot, done here on a $2^8 x 2^8$ pixel grid, the height (in the vertical) of the structures represents also the values of energy $\varepsilon$ and concentration $\rho$. The transformation from the former to the latter field needs another fractional integration (filter $k^{-1.33}$).

discussion). To model such processes, the obvious method to proceed is by replacing the unit Gaussian $u_{\underline{k}}$ in eq. 3.3 by a unit Lévy denoted $u^{(\alpha)}$). However, since the model is constructed by exponentiating these noises in real space, and must satisfy $\langle \varepsilon_\lambda \rangle = 1$, the probability distribution of positive real space noises $u_{\underline{x}}^{(\alpha)}$ must decay at least exponentially fast so that we obtain finite moments of positive order. This requires use of "extremally" asymmetric Lévy distributions. In such distributions, the extreme negative values decrease very slowly as $|u_{\underline{x}}^{(\alpha)}|^{-\alpha}$ however, the probability distribution for extreme positive values is quite different, it decays as $\exp(-|u_{\underline{x}}^{(\alpha)}|^{\alpha'})$ where $1/\alpha+1/\alpha'=1$. Large negative values of $u_{\underline{x}}^{(\alpha)}$ are so frequent that the random variable obtained after exponentiation ($\exp(u_{\underline{x}}^{(\alpha)})$) is very nearly 0, and all negative moments diverge. We shall see that in the cascade model this has the effect of producing frequent deep "holes" or very weak regions; Lovejoy and Schertzer (this volume) suggest on this basis that this makes these simulations promising as cloud models (their analysis of satellite data yields $\alpha \sim 0.63, 1.7$ for visible ansd infrared channels respectively).

The procedure for producing Lévy clouds therefore differs from the Gaussian case in that (appropriately normalized) extremal (white) noises must be produced in real space, and transformed into Fourier space to yield appropriate random variables $u_{\underline{k}}^{(\alpha)}$. Once this Lévy "sub-generator" field has been produced, we proceed as in the Gaussian case, except that we now require a filter $f(\underline{k}) = |\underline{k}|^{-d/\alpha'}$. The transition from $\alpha$ to $\alpha'$ is a consequence of passing from real to Fourier space. The extremal Lévy variables can be obtained by convergent sums of a large number of negative hyperbolic variables (see appendix B for details on the correct normalization).

The physical interpretation of the result of using such variables is straightforward: we are still multiplicatively creating Gaussian "mountains" but now they are pierced by strong Lévy-stable "holes" created by the exponentiation of occasional large negative values. Figure 8 shows a two dimensional illustration of two examples of subgenerator field used in continuous multiplicative cascades. The field at the top is made of unitary (mean=0, variance=1) symmetric Gaussian ($\alpha$=2) white noises. At the bottom the field is obtained by sums of centered asymptotically hyperbolic random variables converging towards asymmetrically negative Lévy-stable white noises (mean=0, $\alpha$=1.6). The perspective plots of the field are depicted on the same physical space, using a $2^8 \times 2^8$ pixel grid. The height (in the vertical) of the structures represents respectively the values of the associated random variables, here uniformly independently distributed (the lengths of the appearing vertical axes provide a reference unit).

Once the (real space) subgenerator field is obtained as in fig. 8 (bottom) using the normalization in appendix B, we produce the 1/f Lévy noise by effecting a fractional integration as described in section 3.3 except that we now use here the filter $k^{-d/\alpha'}$ ($d/\alpha' = d - d/\alpha = 0.75$, if $d$=2 and $\alpha$=1.6 as in figures 9a and 9b). We then exponentiate the resulting field and normalize by dividing by $c_N$ from eq. B.14. Figures 9a and 9b illustrates two such fields having different resolutions: respectively 128x128 and 256x256. Both fields have a first order moment codimension $C_1$=0.8. The cloud water concentration fields are obtained in the same way as for the Gaussian case by taking 1/3 powers and a (second) fractional integration. In figure 9a, the passive scalar distribution (bottom) features a hierarchy of structures having different intensities, and figure 9b (bottom), which was based on the subgenerator field of fig. 8 (bottom), has a dominant structure in the back corner which appears to be the random result of a low clustering in that region of the negative values of the subgenerator, so that their broad attenuating effect is almost absent even if the multiplicative aspect of small structures "growing" on this "mountain" is still clearly evident. The clustering influence is not surprising since the passage from the subgenerator to the generator invokes, as well, a scale invariant smoothing operation (fractional integration) which do not alter the phases of the well localized negative Lévy-stable increments of the subgenerator but allows to group their influence in clusters since the fractional integration scatters the effect of given increments onto their neighbourhoods (the same argument applies for positive exponential increments or for symmetric values in the Gaussian case).

## 4. CONCLUSIONS

We have shown how passive scalar clouds, featuring scaling and intermittency, can be modeled by fractional integration over appropriate powers of conserved but highly intermittent multifractal fluxes. In order to produce multifractal (multiple scaling) fields, we show that it is sufficient to create a field whose logarithm is a "1/f noise". Such fields can be readily produced in Fourier space using either Gaussian or Lévy generators (white noises with Gaussian or (extremal) Lévy distributions with random phases and appropriate

power law filters). Just as the latter are the basic universality classes for the addition of random variables, the mulifractal fields they generate form the universality classes of multiplicative processes. Unlike the cascade processes most often discussed in the literature, the cascades produced here are "canonical" in the sense that energy flux is conserved only on average rather than for each realization and at each scale[1]. Aside from being physically more realistic (since it treats eddies at each scale as open rather than closed systems), canonical cascades have the advantage of lending themselves relatively easily to a continuous Fourier treatment. In contrast, the rigid constraints placed on the cascade at each step (and everywhere in space) in the microcanonical case cannot easily be imposed in Fourier space, hence the of construction of continuous microcanical cascades is far more difficult. All parts of the simulations described here were reentrant and recursive allowing an unlimited number of downward and upward zooms. The physical basis is provided by the multiplicative character of the cascade simulating the breaking of eddies due to nonlinear interactions or internal instabilities, and also by scaling and intermittency, which is of broadly the same sort as that specified by the dynamical (nonlinear, partial differential) equations. Because of the possibility of "zooming", these models are effectively capable of examining turbulent fields at arbitrarily high resolution and may be expected to be indispensable in modelling fully developed turbulence.

These models have many possible applications; particularly in remote sensing, hydrology and meteorology since explicit stochastic models of broadly this type are required for solving basic problems in measurement, calibration and forecasting. Even in the (unusual) case where measuring devices directly sense signals linearly proportional to the quantity of interest, the sub temporal/spatial resolution fluctuations will not be easy to take into account because of the fundamental distinction between the "bare" and "dressed" cascade quantities. In the more usual case (such as radar or satellite remote sensing of rain and clouds), the instruments measure a (radiation) field which is non-linearly related to that of interest, hence explicit subresolution modelling is imperative. In both cases, the multifractal nature of the underlying field will lead to resolution dependent measurements which are of little intrinsic value since they depend mainly on the sensor rather than the characteristics of the field under study. We view the development of multifractal stochastic models as an essential component in developing scale invariant approaches two the problem of remote sensing; see Davis et al. (this volume).

As far as numerical weather prediction is concerned, one may divide applications into two categories. First there are a number of applications which involve evaluating the "stochastic coherence" (Schertzer et al., 1983) of the models i.e. do any of the steps proceeding from analysis, initialization to numerical integration artificially break the scaling and/or attenuate extreme fluctuations (such as meteorological fronts)? This question is directly related to the types of ("coherent") structures produced in the NWP models and in multifractal cascades. A further, related problem that can be studied with the help of cascade processes is the problem of predictability and its limits as well as developing procedures for stochastic forecasting.

A second category of applications is more theoretical - how can the stochastic cascade generator be related to the dynamical equations? This is likely to be the key problem in any clean "renormalization" (i.e. sub-grid parametrisation of the model equations. Since the addition of other fields (such as radiation, humidity, etc.) coupled non-linearly with the basic dynamical equations will introduce new conserved fluxes, we may expect the true system of non-linear partial differential equation governing the atmosphere to be described by coupled cascade processes and to share many of the basic properties (multiple scaling, intermittency) discussed here. In this regard, the universality classes predicted by continuous cascade models provides promise for great simplifications.

## APPENDIX A: SUMMARY OF DISCRETE MULTIPLICATIVE CASCADES: THE $\alpha$- AND $\beta$-MODELS

The basic idea of dynamical cascade models is that the structures at neighboring scales modulate each other in a multiplicative way, simulating the breaking of eddies (and consequent transfer of energy fluxes to smaller scales) due to nonlinear interactions and internal instabilities. The original idea, goes back to

[1]This is "microcanonical" case which in the small scale limit involves the extraordinarily restrictive property of conservation of flux at each point in space; see Schertzer and Lovejoy (this volume).

Richardson, but has evolved considerably especially since the impetus of Kolmogorov's (1962) suggestion that intermittency involves log-normally distributed fluxes.

The cascade is built with respect to the energy-flux and passive scalar-flux conservation requirements: $<\varepsilon>=1$ and $<\chi>=1$. The basic procedure for producing discrete cascades is as follows: starting from the outer scale $l_0$ with unit density of energy flux, representing a primitive uniform eddy, we pass to smaller scale sub-eddies ($\lambda$ times smaller, where in discrete cascades, $\lambda$ must be an integer >1) by breaking the eddy, transfering the energy flux to the $\lambda^d$ sub-eddies (d is the dimension of space in which the process occurs).

Various energy flux redistribution mechanisms have been proposed in the literature, the interesting cases being stochastic. The simplest of these is the "$\beta$ model" in which energy fluxes are modulated by random factors $\mu\varepsilon$ chosen from a binomial process such that for each sub-eddy:

$$\begin{aligned} &Pr(\mu\varepsilon=\lambda^C) = \lambda^{-C} \\ &Pr(\mu\varepsilon=0) = 1-\lambda^{-C} \end{aligned} \qquad (A.1)$$

As the cascade proceeds to smaller and smaller scales, the energy flux is concentrated in smaller and smaller regions while conserving the ensemble average flux $<\varepsilon>=1$, ultimately becoming a singularity of order C over fractal sets (codimension C). Many ways of generalizing this process exist; the simplest is the "$\alpha$ model"[1] in which the above "dead"/"alive" choice is replaced by "active/"weak":

$$\begin{aligned} &Pr(\mu\varepsilon=\lambda^{C/\alpha}) = \lambda^{-C} \\ &Pr(\mu\varepsilon=\lambda^{-C/\alpha'}) = 1-\lambda^{-C} \end{aligned} \qquad (A.2)$$

The $\alpha$ model yields multifractal rather than monofractal measures (Schertzer and Lovejoy, 1983), and is thus far more interesting. More recently, "random $\beta$ models" in which the parameter C is chosen randomly (Benzi et al., 1984), and with certain (complex) correlations (Siebsema et al., 1988) have been proposed. The latter models were also subjected to an additional (very restrictive) constraint that the energy flux be exactly conserved everywhere in space and at each scale, i.e.:

$$\sum_{i=1}^{\lambda^d} \mu\varepsilon_i = \lambda^d \qquad (A.3)$$

for the sum of the random factors $\mu\varepsilon_i$ over each of the $\lambda^d$ subeddies at each step. In analogy with the statistical physics of energy fluctuations (rather than energy *flux* fluctuations), cascades subjected to this constraint (which induces subtle correlations between the previously independent $\mu\varepsilon_i$) are called "microcanonical" (see below), whereas the $\alpha$ and $\beta$ models are canonical"- they only conserve the fluxes on average. Recently, Meneveau and Sreenivasan (1987) baptized the microcanonical $\alpha$ model the "p model". To produce discrete versions of the universal continuous cascades discussed in the text, $\mu\varepsilon$ must be taken as either log-normal ($\alpha=2$), or log-Lévy ($\alpha<2$).

One of the distinguishing features of microcanonical cascades is that unlike its canonical counterpart, averages of moments over completed cascades (dressed moments, see below and Lavallée et al., this volume), over sets with dimension d, always converge. Although this seems to be one of the reasons for the popularity of microcanonical models, it is not compelling, particularly since averages over sets with dimension arbitrarily close to d (but less) feature divergence and most of the other properties of the canonical models.

## APPENDIX B: PRODUCING EXTREMAL LÉVY VARIABLES

Lévy variables generally have probability distributions of the form $Pr(>x) \sim |x|^{-\alpha}$ ($\alpha<2$) for sufficiently large absolute values of the random variable x. Extremal Lévy variables are special cases in which the algebraic tail is confined to either the positive or negative extremes only - the other tail will be generally $\exp(-|x|^{\alpha'})$ where $1/\alpha+1/\alpha'=1$. Extremal Lévy variables are required for convergence of the Laplace

[1]Note that this $\alpha$ is quite different from $\alpha$ in the Lévy distribution used in the body of this paper.

characteristic function (eq. 3.4) and hence for generating cascades with $\alpha<2$. Below, we describe how to produce such cascades including the correct normalization.

Consider w as a uniform random variable in the interval [0,1] (efficient numerical routines are readily available for generating these). The variable $y' = w^{-1/\alpha}$ will therefore have the density:

$$p(y') = \alpha y'^{-1-\alpha} \quad y' \geq 1 \qquad = 0 \quad y'<1 \tag{B.1}$$

The central limit theorem (see in Schertzer and Lovejoy (this volume) for discussion) ensures that summing n independent variables p(y) will approach a Lévy limit distribution parameter $\alpha$ when n tends to infinity.

We now seek the correct centering and normalization constants $\mu$ and $\xi$ such that an extremal Lévy will result in the large n limit. Consider the normalized and centered variable:

$$y = \xi(\mu - y') \tag{B.2}$$

Its second Laplacian characteristic function $\varphi_y(h)$ is given by;

$$e^{\varphi_y(h)} = \langle e^{yh} \rangle = e^{\xi\mu h} \alpha \int_1^\infty e^{-\xi h y'} y'^{-1-\alpha} dy' \tag{B.3}$$

$$e^{\varphi_y(h)} = \alpha e^{\xi\mu h} \xi^\alpha \Gamma(-\alpha, \xi h) \tag{B.4}$$

where $\Gamma$ is the incomplete gamma function:

$$\Gamma(\nu, x) = \int_x^\infty e^{-t} t^{\nu-1} dt \tag{B.5}$$

and furthermore:

$$\Gamma(-\alpha, x) \approx \Gamma(-\alpha) + \frac{x^{-\alpha}}{\alpha} + \frac{x^{-\alpha+1}}{1-\alpha} - \ldots \tag{B.6}$$

Hence:

$$e^{\varphi_y(h)} = (1 + \xi\mu h + \frac{(\xi\mu h)^2}{2!} + \ldots)(1 + \frac{\alpha\xi h}{1-\alpha} + \alpha\Gamma(-\alpha)(\xi h)^\alpha + \ldots) \tag{B.7}$$

$$e^{\varphi_y(h)} = 1 + \xi h(\mu - \frac{\alpha}{\alpha-1}) + \alpha\Gamma(-\alpha)(\xi h)^\alpha + \ldots$$

Hence, taking:

$$\mu = \frac{\alpha}{\alpha-1} \tag{B.8}$$

we obtain:

$$e^{\varphi_y(h)} = \langle e^{yh} \rangle = 1 + \alpha\Gamma(-\alpha)(\xi h)^\alpha + \ldots \tag{B.9}$$

Hence:

$$\langle \exp\{\frac{h}{n^{1/\alpha}} \sum_{i=1}^{n} y_i\} \rangle = (1 + \alpha\Gamma(-\alpha)\frac{(\xi h)^\alpha}{n} + \ldots)^n \rightarrow \exp(\alpha\Gamma(-\alpha)(\xi h)^\alpha) \tag{B.10}$$

Thus for large n, the random variable:

$$Y = \frac{1}{n^{1/\alpha}} \sum_{i=1}^{n} \xi\left(\frac{\alpha}{\alpha-1} - w_i^{-1/\alpha}\right) \tag{B.11}$$

has (Laplacian) characteristic function:

$$\langle e^{Yh} \rangle = \exp(\alpha\Gamma(-\alpha)(\xi h)^{\alpha}) \tag{B.12}$$

Hence, since the (unnormalized) scaling exponent $K_u(h) = C_1 h^{\alpha}\alpha'/\alpha$, (subscript "u" for unnormalized) we must choose $\xi$ so that:

$$\xi^{\alpha} = \frac{C_1\alpha'}{\alpha^2\Gamma(-\alpha)} \tag{B.13}$$

or, using the identity $\Gamma(2-\alpha)=\Gamma(-\alpha)(-\alpha)(1-\alpha)$ and the fact that $1/\alpha'+1/\alpha=1$, we obtain:

$$\xi = \left(\frac{C_1}{\Gamma(2-\alpha)}\right)^{1/\alpha} \tag{B.14}$$

furthermore, the resulting field must be normalized by dividing by $\lambda^{K_u(1)}$, i.e.

$$c_N = \lambda C_1\alpha'/\alpha \tag{B.15}$$

yielding a normalized field whose scaling exponent is:

$$K(h) = K_u(h) - hK_u(1) = \frac{C_1\alpha'}{\alpha}(h^{\alpha}-h) \tag{B.16}$$

In summary, to obtain extremal Lévy variables which will generate cascades with parameters $\alpha, C_1$, we produce a large number[1] (n) of uniform random variables w, and hyperbolic variables $y' = w^{-1/\alpha}$. We then transform this into a new (centered, normalized) random variable y using equation B.2 with centering and norming constants given by B.8, B.14. We sum n of these, and normalize with $n^{1/\alpha}$ as in eq. B.11. The result is an extremal Lévy random variable with the required properties.

ACKNOWLEDGMENTS

We acknowledge fruitful discussions with J.P. Kahane, P. Ladoy, A. Davis, P. Gabriel, A. Saucier, G. Sarma, Y. Tessier, P. Brenier and R. Viswanathan.

REFERENCES

Benzi , R., G. Paladin, G. Parisi, A. Vulpiani, 1984: J. Phys., A17, 3521.

Davis, A., S. Lovejoy, D. Schertzer, 1990: Radiative transfer in multifractal clouds. (this volume).

Kolmogorov, A. N., 1962: A refinement of previous hypothesis concerning the local structure of turbulence in viscous incompressible fluid at high Reynolds number. J. Fluid Mech., 13, 82-85

Lavallée, D., D. Schertzer, S. Lovejoy, 1990: On the determination of the co-dimension function. (this volume).

[1]The number required for convergence can be quite large, and increases as $\alpha$ approaches 2. For example, for $\alpha$=1.5, it was found that n ≈30 was required.

Lovejoy, S., D. Schertzer, 1990: Multifractal analysis techniques and the rain and cloud fields from $10^{-3}$ to $10^{-6}$m. (this volume).

Mandelbrot, B, 1972: in Statistical models of turbulence, Lecture notes in physics, 12, eds. M. Rosenblatt and C. Van Atta, Springer Verlag, p. 333.

Mandelbrot, B., 1988: An introduction to multifractal distribution functions. Fluctuations and pattern formation, eds. H.E. Stanley and N. Ostrowsky, Kluwer.

Meneveau, C., K.R. Sreenivasan, 1987: Simple multifractal cascade model for fully developed turbulence, Phy. Rev. Lett., 59, 1424-1427.

Obukhov, A., 1962: Some specific features of atmospheric turbulence. J. Geophys. Res, 67, 3011-3014.

Parisi, G., U. Frisch, 1985: A multifractal model of intermittency, Turbulence and predictability in geophysical fluid dynamics and climate dynamics, 84-88, Eds. Ghil, Benzi, Parisi, North-Holland.

Schertzer, D., S. Lovejoy, G. Therry, J. Coiffier, Y Ernie, and J. Clochard, 1983: Are current NWP system stochastically coherent? Preprints, IAMAP/WMO Symp. Maintenance of the Quasi-Stationary Components of the Flow in the Atmosphere and in Atmospheric Models, Paris. WMO, Genrva, 325-328.

Schertzer, D., S. Lovejoy, 1987a: Singularités anisotropes, et divergence de moments en cascades multiplicatifs. Annales Math. du Qué., 11, 139-181.

Schertzer, D., S. Lovejoy, 1987b: Physically based rain and cloud modeling by anisotropic, multiplicative turbulent cascades. J. Geophys. Res., 92, 9692-9714.

Schertzer, D., S. Lovejoy, 1990: Scaling nonlinear variability in geodynamics: Multiple singularities, observables and universality classes. (this volume).

Siebsema, A.P., R. R. Tremblay, A. Erzan, 1988: Multifractal cascades with interactions. (Preprint).

Wilson, J., S. Lovejoy, D. Schertzer, 1986: An intermittent wave packet model of rain and clouds. 2nd conf. on satellite meteor. and remote sensing, AMS, Boston, 233-236.

Where[1] $P(\nabla) = \nabla^{-2}\nabla_i\nabla_j$. First we note that the nonlinear terms $((1-P(\nabla))\ \underline{v}\cdot\nabla\ \underline{v}\ ,\ \underline{v}\cdot\nabla\ \rho)$ of both the incompressible Navier-Stokes equations and the equation of (passive) advection dynamically conserve the fluxes of energy and scalar variance (having densities $\varepsilon$ and $\chi$ respectively). This conservation is simply expressed in terms of the fluxes of energy and scalar variance:

$$\varepsilon = -\,\partial\langle v^2\rangle/\partial t = \text{constant}$$
$$\chi = -\,\partial\langle \rho^2\rangle/\partial t = \text{constant} \qquad (2.2)$$

Furthermore, in Fourier space the non-linear terms are heavily weighted to interactions involving neighboring wavenumbers- thus the energy flux is mainly transfered from one scale to a neighboring scale, hence the Richardson- Kolmogorov idea of energy cascading from large to small scales. From here, various phenomenological arguments (which boil down to dimensional analysis) leads to the well-known Kolmogorov scaling (power law) spectra. These all rely on the invariance of the equations under the dilation transformation $\underline{x}\to\underline{x}/\lambda$, $\underline{v}\to\underline{v}/\lambda^H$ and $\rho\to\rho/\lambda^{H'}$ (here and below, the prime refers to the passive scalar cascade). This scaling leads to the following relations for the "fluctuations" at scale $l$ of the fields $\underline{v}$ and $\rho$ (these fluctuations can be characterized for example by the standard deviations of the differences, or increments in v and $\rho$ at points separated by distance $l$) denoted $\Delta v(l)$ and $\Delta\rho(l)$. Furthermore, dimensional analysis applied to $\chi$ and $\varepsilon$ implies H=H'=1/3, or:

$$\Delta v(l) \approx \varepsilon^{1/3}\, l^{1/3}$$
$$\Delta\rho(l) \approx \varphi^{1/3}\, l^{1/3} \qquad (2.3)$$

This invariance leads to power law spectra $E_v(k) \sim k^{-\beta}$ and $E_\rho(k) \sim k^{-\beta'}$ which are respectively the power spectra for the velocity and passive scalar fields (depending on k, the wave number: $k\approx 2\pi/l$) and $\beta=2H+1$ and $\beta'=2H'+1$ since the power spectrum is the Fourier transform of the autocorrelation function:

$$E_v(k) \approx \varepsilon^{2/3}\, k^{-5/3}$$
$$E_\rho(k) \approx \varphi^{2/3}\, k^{-5/3} \qquad (2.4)$$

where $\varphi = \chi^{3/2}\,\varepsilon^{-1/2}$ is the flux resulting from the nonlinear interactions of the velocity and water. Note that the above are scale invariant since their forms are conserved under the dilation $k\to k\lambda$).

The values H=H'=1/3 and $\beta=\beta'=5/3$ were obtained only because the first (h=1) moment of the flux is conserved. So, the question arises as to what should be the scaling exponents for the orders $h\neq 1$. And as far as scale invariance of equations 2.1 is concerned, a different value is possible for every (integer or non integer order) moment hence the terminology of "multiple scaling". This can be expressed for local density values of the field, called (which, at homogeneity scale $l$) with the following scaling laws:

$$\langle \varepsilon_l^h \rangle \sim l^{-(h-1)C(h)}$$
$$\langle \chi_l^h \rangle \sim l^{-(h-1)C'(h)} \qquad (2.5)$$

It can be shown that in general the functions C(h)=d-D(h) and C'(h)=d-D'(h) are codimension functions[2], where D(h), D'(h) are the general multifractal dimensions of the various moments of the process. In the simplest case of a process having a unique fractal codimension C(1), all the various moments of the physical quantities have scaling exponents which are linearly related (differing only by the factor (h-1)), and in this restrictive situation all moments scale the same way. Aside from this, when the functions C(h) and

[1]This form of the equations is obtained after the pressure term is eliminated under the assumption of incompressibility.

[2]A co-dimension is the difference between the dimension d of the embedding space and the fractal dimension of the set of interest.